Reprinted from the **Workshop on Polar Processes and Climate Change,** 13-15 November, 1996, Cancun, Mexico, American Meteorological Society, Boston, MA.

5.4 SATELLITE MICROWAVE RADAR OBSERVATIONS OF CLIMATE-RELATED SEA-ICE ANOMALIES

Mark R. Drinkwater *
Jet Propulsion Laboratory, California Institute of Technology
Pasadena, California

1. INTRODUCTION

Since 1991 a number of international satellites have collected microwave radar image data over Arctic and Antarctic sea ice. The recent successful launch of the ADEOS I satellite, with the NASA NSCAT instrument, also enables additional weather-independent global sea-ice radar data to be acquired and archived in the US. With its pair of 500 km-wide parallel swathes, this radar scatterometer is capable of acquiring data over the entire polar oceans in less than 1 day.

The advantages which scatterometer data offer over 25 km resolution, shorter-wavelength passive microwave instruments such as SSM/I are that sea-ice data retrieval is not limited by atmospheric water vapor content, and also that they approach a higher resolution (~8-10 km at high latitudes) with new imaging techniques (Drinkwater et al., 1993). Together with complementary high resolution (100 m) Synthetic Aperture Radar (SAR) microwave imaging, these frequent repeat data provide a powerful tool for addressing large-scale spatio-temporal sea-ice variations which directly influence and/or respond to polar climate.

Continuous satellite radar data records dating from 1991 until the present day (from ERS-1, ERS-2, and NSCAT), and future approved satellite missions lasting well into the next century, make these data invaluable for addressing interannual variability in sea-ice attributes. Whereas radiometer images provide a valuable historical perspective on sea-ice extent and concentration, tracking of ice kinematics using scatterometer images enables dynamic source and sink terms to be directly addressed in relationship to synoptic-scale ocean and atmospheric forcing. In the following sections, brief examples illustrate how these data are being coupled with dynamic-thermodynamic sea-ice model simulations in studies of interannual variability in sea-ice dynamics.

* Corresponding author address: Dr. Mark R. Drinkwater, Jet Propulsion Laboratory, Mail Stop: 300-323, 4800 Oak Grove Dr., Pasadena, CA 91109; email: mrd@pacific.jpl.nasa.gov

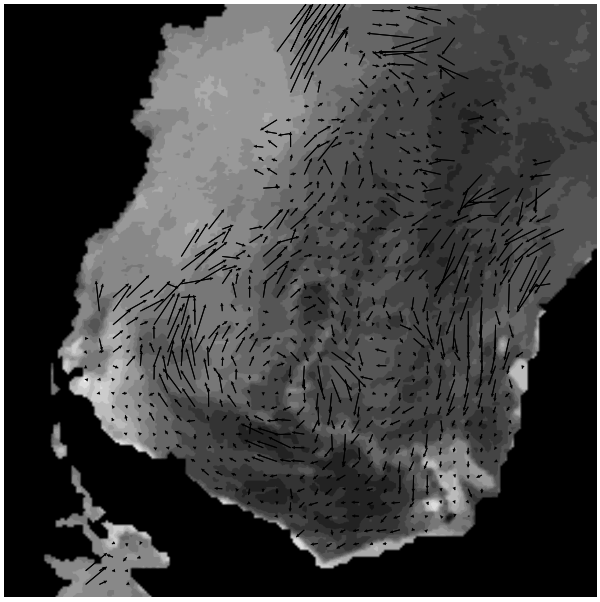

Fig. 1. Sea-ice motion field in the Weddell Sea, Antarctica between days 273 and 276, 1996 [courtesy R. Kwok - JPL], overlaid on image 273.

2. LARGE-SCALE KINEMATICS

Automated algorithms, originally developed for use at the Alaska SAR Facility on SAR images [Kwok *et al.*, 1990], have been adapted for use with ERS and NSCAT images. Correlation of features in "pairs" of images, spaced at intervals of 3-days, enables tracking of ice displacement. Each gridded displacement field is converted into a 3-day mean velocity product as in Fig. 1. In this NSCAT example, sea-ice extent is delineated by the boundary with the masked (black) ocean along the left border. Land and continental ice is similarly masked with the Antarctic peninsula forming the black finger of land in the lower left corner of the image. The 0° meridian runs along the right border of this NSCAT image.

Vector arrows in Fig. 1 indicate scaled velocity and imply a large-scale cyclonic ice circulation which traces the Weddell Gyre. Inflow occurs in the east along the coastline of Antarctica and the northward limb transports ice out along the east coast of the Antarctic peninsula. Ice drift turns sharply near the tip of the peninsula, accelerating eastwards in the Antarctic circumpolar current near the ice margin. Embedded within the western part

of the gyre circulation is a large eddy which has wound a loop of relatively darker seasonal ice eastward toward the central Weddell Sea.

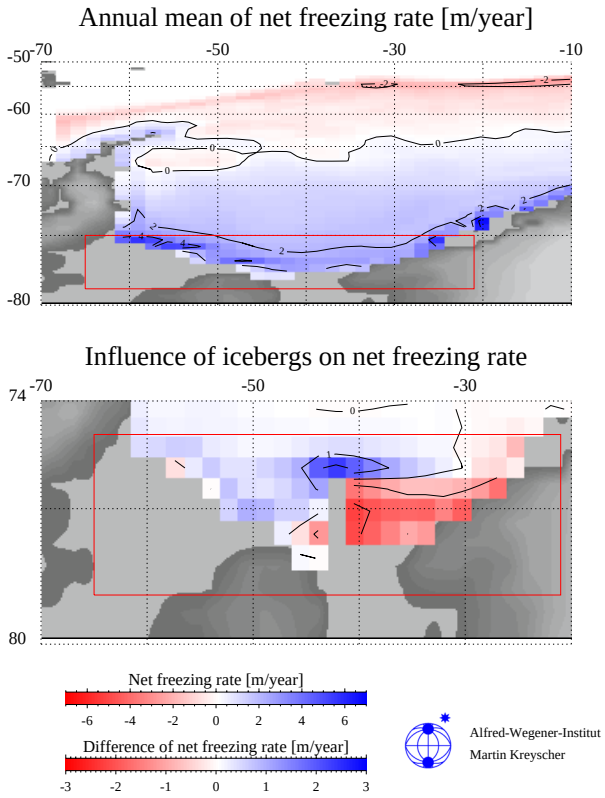

Fig. 2. (a) Regional variability in simulated annual mean Weddell Sea ice production; and (b) net difference in ice production as a function of the grounded icebergs north of the Filchner ice shelf. The enlarged box indicates the region of focus (courtesy M. Kreyscher, AWI).

3. SPATIAL VARIABILITY

Considerable variability in regional ice production can be introduced as a function of time, as a consequence of abrupt changes in the sea-ice dynamics. Large grounded icebergs in Antarctica, for instance, are semi-permanent features which not only redirect ice mass flux but can also have considerable impact on the ocean-ice-atmosphere system through their effect on freshwater flux. Two large icebergs (A23 and 24) which broke away from the Filchner ice shelf and grounded in the1980's, impede inflow of sea ice into the south-western corner of the Weddell Sea. These icebergs are recognized as the bright patches of stationary ice in the lower right corner of Fig. 1. Effects of this artificial peninsula have been simulated in Fig. 2 with a coupled dynamic-thermodynamic model forced using ECMWF wind and temperature fields (between 1986 and 1993). The upper panel indicates mean annual net freezing rate (NFR) without a barrier. In this standard case, polynyas along the coast and ice-shelves dominate ice production, particularly in locations of persistent divergence. In the lower panel of Fig. 2, a realistic barrier was added to the coastline in the location of the icebergs and the difference in net freezing rate calculated. To its east, the perennial or fast-ice cover developing around the stationary icebergs limits ocean-atmosphere fluxes, reducing annual ice production by up to 3 m. In contrast, to the west ice production in the lee polynya is enhanced slightly by 1-2 m/year.

4. INTERANNUAL VARIABILITY

Sea-level pressure and meridional wind fields in the Southern Ocean reveal significant interannual variability on timescales of several years (White and Peterson, 1996). Since the seasonal sea-ice cover surrounding the continent of Antarctica, forms a contiguous pathway for propagation and transfer of climatological anomalies around the globe, it is suggested that these variations should also induce dynamic and thermodynamic adjustments in the sea-ice cover which are both visible in satellite images and model simulations.

Variations in ice production resulting from adjustments to forcing were investigated using the same model described above (Drinkwater and Kreyscher, submitted). Simulation results from the highlighted box in Fig. 2 indicate marked seasonal and interannual variability in ice divergence, as a function of the basin-wide ice circulation and resulting northwards ice drift. Fig. 3 indicates that peaks in mean annual meridional wind velocity (positive = northwards) correspond with peaks in simulated mean annual NFR. Poor model initial conditions for the ice-thickness distribution result in unrealistically high ice growth in 1986 [see (+)], but since most ice is annually swept out of the Weddell Sea basin, the model quickly attains equilibrium in 1-2 years to reproduce the expected interannual variability.

During the period of forcing, a peak in mean annual ice production occurs in 1988 and 1989, in response to enhanced equatorward winds. This cycle corresponds closely with variability observed by White and Peterson (1996). Open water fraction (OWF) records derived from SSM/I passive-microwave images similarly indicate enhanced divergence and creation of open-water during these peak ice-production years. A subsequent 7-year minimum in OWF is observed

in 1991 (Drinkwater and Kreyscher, submitted). Not surprisingly, this corresponds with reduced meridional wind velocities, sluggish northwards ice transport and thus reduced net ice production in the ice-shelf polynya system (shown in Fig. 2).

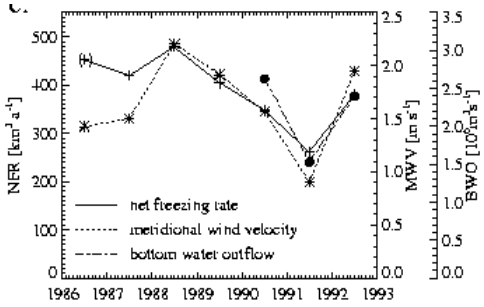

Fig. 3. Interannual variability in annual mean quantities of simulated Net Freezing Rate and ECMWF Meridional Wind Velocity in the box region in Fig. 2; and Bottom Water Outflow at Joinville Island.

Though short, an additional measurement record of Bottom Water Outflow (BWO) at Joinville Island is shown in Fig. 3 [after Fahrbach *et al.*, 1995]. Three annual mean values computed from this seasonal dataset also indicate a clear minimum in 1991, with significant interannual variations of 1.5 Sv. in amplitude. Since this fluctuation requires considerable interannual variation in source water masses, it is suggested that bottom water formation is closely linked to the production of dense, brine-rich, chilled shelf waters during winter ice growth in the Ronne polynya system. As previously demonstrated in Figures 1 and 2, ice production off the Filchner ice shelf is currently limited by convergent, perennial sea ice which is trapped around two large grounded icebergs, rather than a divergent polynya system as off the Ronne ice shelf. Thus, dynamics are largely responsible for regulating sea-ice production and focusing it over the broad continental shelf in the Ronne ice-shelf polynya system.

Interannual variations in freezing rate therefore appear to modulate production of the dense shelf 'source-water' mass which ultimately mixes with intermediate and deep water along its northward, downslope path toward Joinville Island prior to registering in the BWO record. Furthermore, a lag observed between the seasonal maxima in NFR and BWO appear consistent with the time taken for the bottom water to flow northwards from their source region of in the southern Weddell Sea, to the current meters at Joinville Island.

5. ICE MOTION CLIMATOLOGIES

Ice-motion climatologies are a valuable way of combining and compiling ice-drift information. A consistent historical database must be constructed with which long-term comparisons can be made. Anomaly cycles can be generated with respect to historical mean seasonal or annual conditions, but their statistical accuracy is dependent largely upon the temporal extent and the sampling frequency of such data. It is proposed, therefore, to develop a continuing archive of ice dynamics data using the above ice-tracking technology.

Combinations of entire years of ice motion from existing ERS scatterometer image data have been used to derive climatological means as an example here. Fig. 4 shows the Weddell Sea 12-monthly mean climatological ice drift for 1992 together with the streamlines of flow. Fig. 4 is the result of spatially interpolating a weighted average of over 100 individual 3-day gridded ice-motion products, each derived by automated tracking of ice parcels in pairs of these scatterometer images.

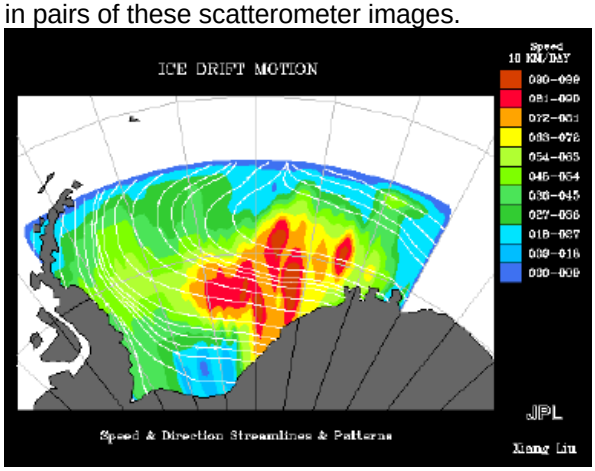

Fig. 4. Weddell Sea 1992 climatological mean ice drift derived from ERS-1 scatterometer 3-day gridded ice motion. White lines indicate streamlines of drift, and the color coding indicates the drift speed in units of 10^1 km/d.

Fig. 4 indicates a large degree of similarity with the mean motion chart interpolated by Kottmeier and Sellmann (1996) from accumulation of sparse temporal and spatial buoy drift records in this region. Streamlines clearly highlight regions of convergence and divergence, while the shaded background image indicates the regions of most rapid or sluggish ice drift.

6. OPEN-OCEAN POLYNYAS

Periods of cyclonic activity and high wind-stress divergence often result in localized fracturing and

lead openings in a sea-ice cover. In late July-early August 1994, storm-induced 'Ekman pumping', and/or drift-induced turbulent mixing at the base of the mixed layer (McPhee et al., 1996), caused a large enough oceanic heat flux to melt and significantly reduce the ice concentration in the vicinity of Maud rise, Antarctica. Notably, this event coincided with a hurricane-force storm which also forced the end of the winter 1994 ANZFLUX experiment in that same location. This intense storm activity resulted in a brief reappearance of the winter Weddell Polynya, lasting a total of about 3 months before disappearing again. Its appearance was first discovered in ERS-1 scatterometer images such as Fig. 5, and confirmed using SAR data acquired in the orbit frame locations shown. These data are presently being analyzed in conjunction with SSM/I passive microwave radiometer data and oceanographic data acquired during the Anzflux experiment [McPhee *et al.*, 1996]. Preliminary findings appear to indicate that the polynya did not survive because deep convection was not initiated.

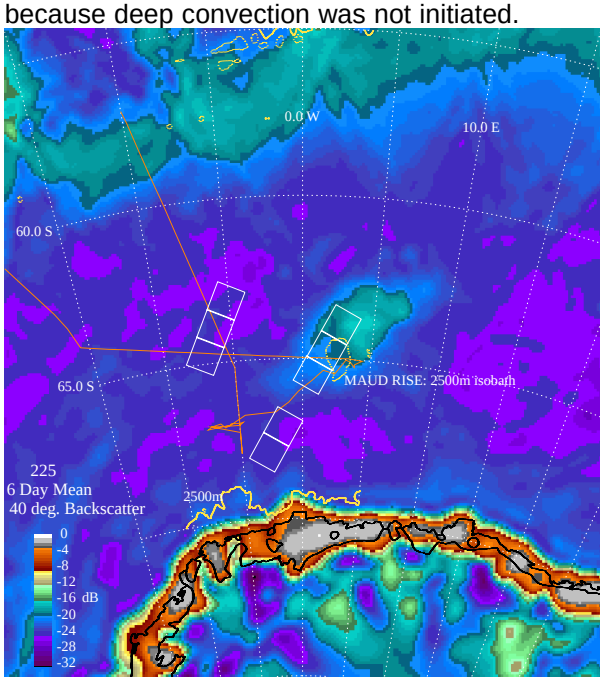

Fig. 5. Winter reappearance of the Weddell Polynya, on day 225, 1994. The 2500 m bathymetric contour indicates the Maud rise.

7. CONCLUSIONS

Global, microwave radar observations are actively revolutionizing the study of polar ocean sea-ice geophysics. Seasonal to interannual changes in global sea-ice drift and accompanying transitions in sea-ice characteristics can now be accurately characterized. Examples linking model simulations with radar remote sensing illustrate how these data can be used to investigate sea-ice not only as a passive receptor for climatic disturbances, but also as a purveyor of climatic anomalies through the ocean-atmosphere system.

Continuing data acquisition will enable a contiguous long-term climatology of more detailed global ice characteristics to be developed. The longer high-resolution satellite radar image records become extended, the better the chances of measuring sea-ice variability associated with climate anomalies on timescales equal to or exceeding the duration of any individual satellite mission. Only then can statistical relationships between forcing and dynamic-thermodynamic response be established on interannual to decadal timescales. These preliminary results only hint at teleconnections between the mid- and high latitude atmospheric and oceanic processes via the sea-ice cover around Antarctica. As the era of microwave remote sensing continues, extended datasets must be widely employed in confirming or denying these preliminary findings via long-term, large-scale observation records of the global sea ice cover.

8. REFERENCES

Drinkwater, M.R., In Press: Satellite Microwave Radar Observations of Antarctic Sea Ice. In C. Tsatsoulis and R. Kwok (Eds.), *Recent Advances in the Analysis of SAR for Remote Sensing of the Polar Oceans*, Springer-Verlag, Chapt. 8.

Drinkwater, M.R., and M. Kreyscher, Submitted: Influence of the Antarctic Circumpolar Wave on Interannual Variability in Weddell Sea Ice Formation and Bottom Water Outflow, *Science.*

Drinkwater, M. R., D. G. Long, and D. S. Early, 1993: Enhanced resolution scatterometer imaging of Southern Ocean sea ice, *ESA Journal*, **17**, 307-322.

Fahrbach, E., G. Rohardt, N. Scheele, M. Schröder, V. Strass, and A. Wisotzki, 1995: Formation and discharge of deep and bottom water in the northwestern Weddell Sea, *J. Mar. Res.*, 53, 515-538.

Kottmeier, C., and L. Sellmann, 1996: Atmospheric and oceanic forcing of Weddell Sea-ice motion, *J. Geophys. Res.*, 101, C9, 20809-20824.

Kwok, R., J.C. Curlander, R. McConnell, and S.S. Pang, 1990: An ice-motion tracking system at the Alaska SAR Facility, *IEEE J. Oceanic Eng.*, OE-15, 1, 44-54.

McPhee, M.G., S.F. Ackley, P. Guest, B.A. Huber, D.G. Martinson, J.H. Morison, R.D. Muench, L. Padman, and T.P. Stanton, 1996: The Antarctic Zone flux experiment, *Bull. Am. Met. Soc.*, 77, 6, 1221-1232.